International Journal of Biomedicine 16(4) (2026) 477-485
http://dx.doi.org/10.21103/Article16(4)_OA3

ORIGINAL ARTICLE

INTERNATIONAL JOURNAL OF BIOMEDICINE

Enhanced Oxidative Phosphorylation Induces Autophagy in Prolactinomas

Yutao Shen[1*]

[1]*School of Nursing, Zhejiang Changzheng Vocational & Technical College, Hangzhou, Zhejiang, China*

Abstract

Background: Currently, there is limited understanding of the relationship between oxidative phosphorylation and autophagy. The microarray data we obtained from prolactinoma samples and normal pituitary samples have revealed enhanced oxidative phosphorylation and autophagy activation in prolactinomas. However, whether autophagy is activated by enhanced oxidative phosphorylation remains unknown.

Methods and Results: Rat prolactinoma MMQ cells were treated with triiodothyronine (T_3) to enhance oxidative phosphorylation, and then autophagy, intracellular reactive oxygen species (ROS), and the expression of RSK1 and its active form, phospho-RSK1, ATG7, and ATG101 were detected. Next, intracellular ROS were eliminated with N-Acetyl-L-cysteine (NAC), and then autophagy and the expression of RSK1, phospho-RSK1, ATG7, and ATG101 were detected. Enhancing oxidative phosphorylation in MMQ cells increased ROS levels, and this accumulation activated autophagy by suppressing RSK1 activation and increasing ATG7 and ATG101 expression.

Conclusion: These findings provide a novel perspective that couples oxidative phosphorylation with autophagy, in which ROS play a pivotal role in linking these two biological functions in prolactinomas. **(International Journal of Biomedicine. 2026;16(4):477-485.)**

Keywords: pituitary adenoma, oxygen consumption rate, reactive oxygen species

For citation: Shen Y. Enhanced Oxidative Phosphorylation Induces Autophagy in Prolactinomas. International Journal of Biomedicine. 2026;16(4):477-485. doi:10.21103/Article16(4)_OA3

Introduction

Pituitary adenoma is a common intracranial tumor, accounting for approximately 25% of all intracranial tumors, and approximately 40% of all pituitary adenomas are prolactinomas.[1] Treating these tumors remains a great clinical challenge, especially for drug-resistant prolactinomas and refractory pituitary tumors[1] due to the lack of effective treatment targets and the complicated mechanism of pituitary tumorigenesis. Autophagy has been reported to be involved in tumorigenesis[2] and is considered a treatment target;[3] however, whether and how autophagy affects pituitary tumorigenesis remain to be fully elucidated.

Autophagy is a significant mechanism for maintaining cellular homeostasis by recycling intracellular nutrients and quality-controlling proteins. Tumor cells rely on autophagy for survival because of their active proliferation, altered metabolism, and nutrient-deprived environment.[4] In tumor cells, autophagy can facilitate tumorigenesis by promoting cell proliferation, but it can also suppress tumorigenesis by inhibiting cell survival and inducing cell death.[5,6] ATG7 and ATG101 have been considered as essential molecules for autophagy.[7,8] ATG7 is an E1-like enzyme that activates ATG12; it functions as an E1 enzyme for ATG5-ATG12 conjugation.[9] ATG101 interacts with ULK1 in an ATG13-dependent manner; ATG101 stabilizes ATG13 expression and contributes to ATG13 function by protecting it from proteasomal degradation.[10]

Abnormal metabolism is a hallmark of cancer.[11-13] Although aerobic glycolysis is commonly regarded as the dominant metabolic pathway in cancer cells,(14) recent research suggests that oxidative phosphorylation (OXPHOS) is also utilized by cancer cells.[15-18] Additionally, the effects of mitochondria on cancer cells are well documented,[19-25] suggesting that mitochondria function actively in cancer cells. Studies have shown that respiratory chain complexes I and III in mitochondria are the primary sources of reactive oxygen species (ROS);[26] therefore, actively functioning mitochondria and enhanced OXPHOS usually lead to increased ROS generation, and excess ROS cause many physiological and pathological changes in cells. However, it is unclear whether mitochondrial activity is increased and ROS influence autophagy in human prolactinoma cells.

© 2026 The Author(s). *International Journal of Biomedicine* is published by IMRDC.
This is an open access article under the CC BY-NC-ND 4.0 license.

In this study, we investigated prolactinomas using a microarray and found abnormalities in the autophagy and oxidative phosphorylation pathways. We found that autophagy was activated and that oxidative phosphorylation was enhanced in prolactinomas. Hence, this project was designed to determine the relevance of activated autophagy and enhanced oxidative phosphorylation in prolactinomas.

Materials and Methods

Tissue Samples and Histology

All prolactinoma samples were obtained from the Department of Neurosurgery, Beijing Tiantan Hospital. Fresh tumor tissue samples were immediately snap-frozen in liquid nitrogen and stored at -80°C. All normal pituitary samples were obtained from Tianjin First Central Hospital by organ donation. Fresh normal pituitary samples were also immediately snap-frozen in liquid nitrogen and stored at -80°C. A total of 31 prolactinoma samples and 25 normal pituitary samples were included in the present study, of which 7 frozen prolactinoma samples and 6 frozen normal pituitary samples were subjected to microarray, 15 paraffin-embedded prolactinoma samples and 10 paraffin-embedded normal pituitary samples were subjected to immunohistochemistry, 4 frozen prolactinoma samples and 4 frozen normal pituitary samples were subjected to Western blot, and 5 frozen prolactinoma samples and 5 frozen normal pituitary samples were subjected to respiratory chain complexes I, III and IV activity assays. Informed consent was obtained from all enrolled subjects, and the study was conducted in accordance with the principles of the Declaration of Helsinki.

Total RNA Extraction

Total RNA was extracted and purified using a mirVana™ miRNA Isolation Kit (AM1561, Ambion, USA) following the manufacturer's instructions. An Agilent Bioanalyzer 2100 (Agilent Technologies, USA) was used to obtain an RNA integrity number (RIN) and assess RNA integrity. Only those samples that showed no degradation (2100 RIN $\geq$ 7.0 and 28S/18S $\geq$ 0.7) were used to generate labeled targets.

Microarray Hybridization

Total RNA was amplified and labeled using a Low Input Quick Amp Labeling Kit, One-Color (5190-2305, Agilent Technologies, USA), following the manufacturer's instructions. Labeled cRNA was purified with an RNeasy Mini Kit (74106, QIAGEN, Germany). Each slide was hybridized with 1.65 **µg** of Cy3-labeled cRNA using a Gene Expression Hybridization Kit (5188-5242, Agilent Technologies, USA) in a hybridization oven (G2545A, Agilent Technologies, USA), according to the manufacturer's instructions. After 17 hours of hybridization, slides were washed in staining dishes (121, Thermo Shandon, USA) with a Gene Expression Wash Buffer Kit (5188-5327, Agilent Technologies, USA), following the manufacturer's instructions. Slides were scanned with an Agilent Microarray Scanner (G2565CA, Agilent Technologies, USA) using the default settings (dye channel: green, scan resolution: 5 µm, PMT: 100, 10%, 16 bit). Data were extracted with Feature Extraction software 10.7 (Agilent Technologies, USA). Raw data were normalized by the Quantile algorithm using GeneSpring Software 11.0 (Agilent Technologies, USA).

Bioinformatics Analysis

The Ingenuity Pathway Analysis (IPA) software package (version 9.0, USA; http://www.ingenuity.com) and the Kyoto Encyclopedia of Genes and Genomes (KEGG) were used to identify predominant canonical pathways in prolactinomas.

Immunohistochemistry (IHC)

Fifteen prolactinoma samples and 10 normal pituitary samples were fixed in 10% paraformaldehyde, decalcified in formic acid, and embedded in paraffin. All samples were sectioned at 5 µM and then processed for IHC staining with an anti-LC3B (1:100, 3868, CST, USA) antibody. The slides were placed in a BOND-III apparatus manufactured by Leica Biosystems, a fully automated, random-access, continuous-access slide-staining system that processes IHC tests simultaneously. IHC protocol F was selected on the machine, and 20 min with epitope retrieval was set as the heat-induced epitope retrieval (HIER) parameter. The Bond™ Polymer Refine Detection (DS9800, Leica Biosystems, Germany) was used to detect the primary antibody. The slides were scanned as digital pictures, and the expression was examined using Aperio AT2 (Leica Biosystems, Germany). The results were calculated using Aperio AT2 (Leica Biosystems, Germany) with digital slide viewing software. The staining intensity was stratified on a scale of 0-3 (0 = no staining, 1 = weak, 2 = moderate, and 3 = strong). An H-score was obtained by multiplying the staining intensity with a constant to adjust the mean to the strongest staining [H-score = 3 * (percentage of strong staining); 1.0 (% weak), 2.0 (% moderate), 3.0 (% strong)] to give a score ranging from 0-300.

Respiratory Chain Complex I, III, and IV Activity Assay

Complex I activity was detected using a Complex I Enzyme Activity Microplate Assay Kit (ab109721, Abcam, UK) according to the manufacturer's instructions. Proteins were isolated from 100 mg of fresh tissue and were diluted to the desired concentration. In total, 200 µl of the diluted sample was used. The absorbance was detected at 450 nm using a multimode microplate reader (Tecan, Männedorf, Switzerland). Complex III activity was detected using a Mitochondrial Complex III Activity Assay Kit (K520, BioVision, USA) according to the manufacturer's instructions. Proteins were isolated from 100 mg of fresh tissue and were diluted to the desired concentration. In total, 200 µl of the diluted sample was used. The absorbance was detected at 550 nm using a multimode microplate reader (Tecan, Männedorf, Switzerland). Complex IV activity was detected using a Complex IV Human Enzyme Activity Microplate Assay Kit (ab109909, Abcam, UK) according to the manufacturer's instructions. Proteins were isolated from 100 mg of fresh tissue and were diluted to the desired concentration. In total, 200 µl of the diluted sample was used. The absorbance was

detected at 550 nm using a multimode microplate reader (Tecan, Männedorf, Switzerland).

Cell Culture

The rat pituitary MMQ cell line was purchased from the American Type Culture Collection (ATCC, USA), whose commercial designation is CRL-10609™, and were cultured in F-12K Medium (30-2004, ATCC, USA) supplemented with 15% (v/v) horse serum (16050-122, Gibco, USA) and 2.5% (v/v) fetal bovine serum (10099-141, Gibco, USA) in a humidified incubator at 37°C in 5% (v/v) CO_2. The culture medium was replaced every other day. For triiodothyronine (T_3) stimulation, MMQ cells were treated with 1 nM or 10 nM, or 100 nM T_3 (T2877, Sigma-Aldrich, USA) for 24 hours. For ROS stimulation, MMQ cells were treated with 100 nM T_3 (T2877, Sigma-Aldrich, USA) and 300 μM pyocyanin (ab141099, Abcam, UK) for 24 hours and 1 hour, respectively. One group of MMQ cells was pretreated with 5 mM N-Acetyl-L-cysteine (NAC) (A105422, Aladdin, China) for 2 hours to eliminate intracellular ROS, and the other group of MMQ cells was not treated with NAC. To activate autophagy, MMQ cells were treated with 100 nM rapamycin (ab120224, Abcam, UK) or 10 mM LiCl (C8381, Solarbio, China) for 24 hours. For autophagy inhibition, MMQ cells were treated with 30 μM chloroquine (C193834, Aladdin, China) or 2.5 mM 3-methyladenine (ab120841, Abcam, UK) for 24 hours. For bromocriptine treatment after autophagy activation or inhibition, MMQ cells were treated with 50 μM bromocriptine (S84497, Yuanye Bio-Technology, China) for 48 hours.

Autophagy Detection

MMQ cells were collected by centrifugation and then resuspended to a density of 1 x 10^6/ml. Autophagy in MMQ cells was detected using an Autophagy Detection Kit (ab139484, Abcam, UK) according to the manufacturer's instructions. The fluorescence images were observed and photographed using a fluorescence microscope (Axio Observer. Z1, Zeiss, Germany). The autophagic signal was imaged using a standard FITC filter set, and the nucleus was imaged using a DAPI filter set.

Measurement of Intracellular ROS

After MMQ cells were treated with 1 nM, 10 nM, or 100 nM T_3 for 24 hours, intracellular ROS were monitored using a Cellular Reactive Oxygen Species Detection Assay Kit (ab186029, Abcam, UK) according to the manufacturer's instructions. The fluorescence intensity was detected at E_x/E_m = 650/675 nm using a multimode microplate reader (Tecan, Männedorf, Switzerland).

Mitochondrial Superoxide Detection

After MMQ cells were treated with 1 nM, 10 nM, or 100 nM T_3 for 24 hours, mitochondrial superoxide was detected using a MitoSOX™ Red Mitochondrial Superoxide Indicator (M36008, ThermoFisher, USA) according to the manufacturer's instructions. The fluorescence intensity was detected at E_x/E_m = 510/580 nm using a multimode microplate reader (Tecan, Männedorf, Switzerland).

Oxygen Consumption Assessment

The oxygen consumption rate (OCR) was assessed using an Oxygen Consumption Rate Assay Kit (600800, Cayman Chemical, USA) according to the manufacturer's instructions. The fluorescence intensity was detected at E_x/E_m = 380/650 nm using a multimode microplate reader (Tecan, Männedorf, Zürich, Switzerland). The OCR is the slope of the curve obtained by plotting fluorescence intensity over time.

Protein Extraction and Western Blot Assay

Tissue samples or cells were lysed using RIPA lysis buffer (C1050, Applygen, China) with a protease inhibitor cocktail (P1265, Applygen, China) and a phosphatase inhibitor cocktail (P1260, Applygen, China). The total protein concentration was determined using a BCA Protein Assay Kit (SK258437, ThermoFisher, USA). Equal amounts of total proteins were separated by SDS-PAGE (10% gels) for SQSTM1 (1:1000, 39749, CST, USA), RSK1 (1:1000, 8408, CST, USA), phospho-RSK1 (1:1000, 9335, CST, USA), ATG7 (1:1000, 8558, CST, USA) and ATG101 (1:1000, 13492, CST, USA) detection, and 15% gels were used for LC3B (1:500, 3868, CST, USA) detection. GAPDH was used as the protein loading control. After SDS-PAGE, the proteins on the gels were transferred to BioTrace nitrocellulose membranes (66485, Pall, USA), blocked with 5% skim milk in Tris-buffered saline (TBS, pH 7.4; 20 mM Tris-HCl, 150 mM NaCl), and then incubated with different primary antibodies overnight at 4°C. The following day, the membranes were incubated with IRDye-labeled goat anti-mouse or goat anti-rabbit IgG at room temperature for 1 hour. Finally, the protein bands were scanned using a LI-COR Odyssey system (LI-COR Biosciences, USA). At least 3 independent experiments were performed, and a representative result is shown.

Cell Viability Assay

Cell viability was determined using a Cell Counting Kit-8 (CK04, Dojindo, Japan) according to the manufacturer's instructions. MMQ cells were plated in 96-well plates at approximately 1×10^4 cells per well. After addition of the CCK-8 solution, the plate was incubated at 37°C for 4 hours, and absorbance was measured at 450 nm using a multimode microplate reader (Tecan, Männedorf, Switzerland).

Cell Proliferation Assay

Cell proliferation was determined using a BrdU Cell Proliferation ELISA (11647229001, Roche, Switzerland) according to the manufacturer's instructions. MMQ cells were plated in 96-well plates at approximately 1×10^4 cells per well. After addition the BrdU solution, the plate was incubated at 37°C for 2 hours, and the cells were then fixed for 30 minutes at room temperature. Next, after adding the anti-BrdU-POD solution, the plate was incubated at room temperature for 90 minutes. After Substrate solution and 1 M H_2SO_4 were added to the wells, absorbance was measured at 450 nm using a multimode microplate reader (Tecan, Männedorf, Switzerland).

Measurement of Prolactin Production

The concentration of prolactin in the culture supernatant was measured using a Prolactin ELISA Kit (K4688, BioVision,

USA) according to the manufacturer's instructions. The supernatant was collected from the culture medium. In total, 50 µl of the supernatant was used. The absorbance was detected at 450 nm using a multimode microplate reader (Tecan, Männedorf, Switzerland).

Statistical Analysis

Statistical analyses were performed using GraphPad Prism 7 (San Diego, USA). The data are presented as the mean ± standard error of the mean (SEM). Variables were analyzed using an unpaired Student's t-test to compare two groups, unless indicated otherwise. For all statistical analyses, a p-value < 0.05 was considered statistically significant.

Results

Differentially Expressed Genes are Enriched in the Autophagy and Oxidative Phosphorylation Pathways in Prolactinomas

We observed significant differences in expression between prolactinoma and normal pituitary samples by gene expression microarray analysis. A total of 2,481 genes were significantly differentially expressed in the prolactinoma and normal pituitary samples ($p < 0.05$, fold change > 2). Among these 2,481 genes, 1,001 were upregulated, and 1,480 were downregulated in prolactinoma samples (Supplementary Table 1).

Based on the results of the IPA and KEGG pathway analyses, we found that the genes upregulated in prolactinomas were enriched in the regulation of the autophagy (Figure 1A) and oxidative phosphorylation (Figure 1B) pathways.



Figure 1. *Ingenuity pathway analysis of differentially expressed genes in prolactinomas.*

(A) The genes with upregulated expression are enriched in the regulation of the autophagy pathway. (B) The genes with upregulated expression are enriched in the oxidative phosphorylation pathway. Pink represents most genes with upregulated expression in the pathway, while green represents most genes with downregulated expression in the pathway. The more up- or downregulated genes enriched in the pathway there are, the darker the pink or green color in the grid.

We speculated that autophagy was activated and that oxidative phosphorylation was enhanced in prolactinomas because the genes with upregulated expression directly or indirectly participate in both processes. There were two genes with upregulated expression in the regulation of the autophagy pathway: ATG7 and ATG101 (Supplementary Table 2). We speculated that ATG7 and ATG101 were relevant to the autophagy activation in prolactinomas. We further analyzed the KEGG data and found that the expression of RPS6KA1, also known as RSK1 and involved in the mTOR signaling pathway, was downregulated in prolactinomas (Supplementary Table 1 and Supplementary Table 2). RSK1 functions in the mTOR pathway by directly phosphorylating TSC2, thereby potently inhibiting TSC2's ability to suppress mTOR signaling. (27) We speculated that RSK1 was also relevant to the autophagy activation in prolactinomas.

Autophagy Activation in Prolactinomas

LC3B and SQSTM1 were selected to verify the autophagy activation in prolactinomas. Compared with normal pituitaries, prolactinomas had increased LC3B expression (Figure 2A, 2B) and reduced SQSTM1 expression (Figure 2B). Then, we detected the expression of ATG7, ATG101, RSK1, and its active form, phospho-RSK1, in prolactinomas and normal pituitaries. The results showed that the expression of ATG7 and ATG101 was higher in prolactinomas than in normal pituitaries (Figure 2C), and the expression of RSK1 and phospho-RSK1 was lower in prolactinomas than in normal pituitaries (Figure 2C). These results indicated that autophagy was activated in prolactinomas, and the expression of ATG7, ATG101, and RSK1 was consistent with microarray data.

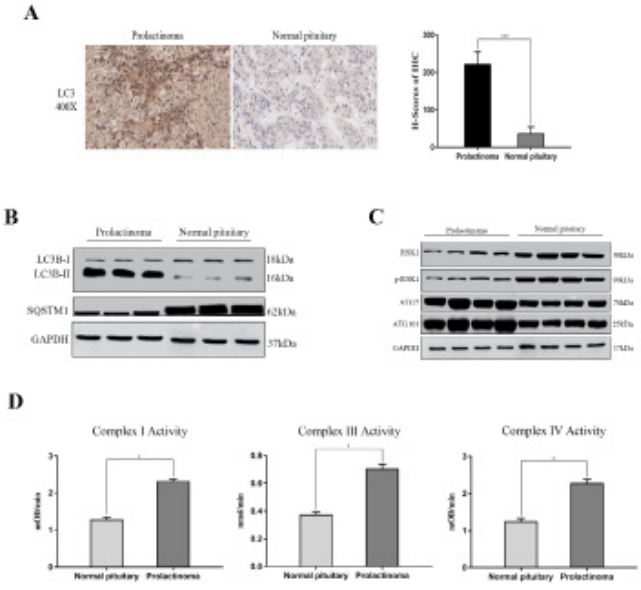


Figure 2. *Validation of microarray data in tissue samples.*

*(A) Immunohistochemistry showed that the expression of LC3 in prolactinomas was higher than that in normal pituitaries (n = 15 for prolactinomas, n = 10 for normal pituitaries). (B) The expression of LC3B-II in prolactinomas was higher than in normal pituitaries. The expression of SQSTM1 in prolactinomas was lower than in normal pituitaries (n = 3 for prolactinomas, n = 3 for normal pituitaries). (C) The expression of RSK1 and phospho-RSK1 in prolactinomas was lower than in normal pituitaries. The expression of ATG7 and ATG101 in prolactinomas was higher than in normal pituitaries (n = 4 for prolactinomas, n = 4 for normal pituitaries). (D) The activity of respiratory chain complexes I, III and IV was higher in prolactinomas than in normal pituitaries (n = 5 for prolactinomas, n = 5 for normal pituitaries). Bars represent the mean of the respective individual ratios ± SEM. *- p<0.05; ***- p<0.001.*

The Increased Activity of Respiratory Chain Complexes I, III, and IV in Prolactinomas

To verify that oxidative phosphorylation is enhanced in prolactinomas, we assessed mitochondrial function by measuring the activities of respiratory chain complexes I, III, and IV. The results showed that the activities of respiratory chain complexes I, III, and IV were higher in prolactinomas than in normal pituitaries (Figure 2D). These results indicated that oxidative phosphorylation was enhanced in prolactinomas.

Enhanced Oxidative Phosphorylation Induces Autophagy and Increases the Expression of ATG7 and ATG101, and Suppresses the Activation of RSK1 in MMQ Cells

To study whether enhanced oxidative phosphorylation induces autophagy in prolactinomas, we used triiodothyronine (T_3) to enhance oxidative phosphorylation and then detected autophagy in MMQ cells. First, to verify that T_3 enhances oxidative phosphorylation in MMQ cells, we measured OCR after treatment with different concentrations of T_3. The results showed that T_3 treatment increases OCR in a dose-dependent manner, suggesting enhanced oxidative phosphorylation in MMQ cells (Figure 3A, 3B). After MMQ cells were treated with 1 nM, 10 nM, or 100 nM T_3 for 24 hours, we directly detected autophagy using an Autophagy Detection Kit. As shown in Figure 3C, the LC3 fluorescence intensity increased with increasing T_3 concentration. Additionally, total protein was extracted from MMQ cells after 24 hours of treatment with different concentrations of T_3, and the expression of LC3B-II and SQSTM1 was detected by Western blot. As shown in Figure 3D, LC3B-II expression increased, while SQSTM1 expression decreased as T3 concentration increased. These results indicated that enhanced oxidative phosphorylation induced autophagy in MMQ cells.

We further assessed the expression of ATG7, ATG101, RSK1, and phospho-RSK1 in MMQ cells after treatment with 1 nM, 10 nM, or 100 nM T_3 for 24 hours. The results showed that the expression of ATG7 and ATG101 increased with increasing T_3 concentration; there was no significant difference in RSK1 expression between groups; and the expression of phospho-RSK1 decreased with increasing T_3 concentration (Figure 3E). These results indicated that enhanced oxidative phosphorylation increased the expression of ATG7 and ATG101 and suppressed RSK1 activation in MMQ cells.

Enhanced Oxidative Phosphorylation Stimulates ROS Generation in MMQ Cells

Electron leakage during electron flow through the electron transport chain produces ROS.(26) To investigate whether ROS production in MMQ cells increases when oxidative phosphorylation is enhanced, we measured cellular ROS levels after cells were treated with 1 nM, 10 nM, or 100 nM T_3 for 24 hours. Compared with cells not treated with T_3, cells treated with T_3 showed increased ROS production, which increased with increasing T_3 concentration (Figure 4A). We also used MitoSOX, a fluorophore that is activated by mitochondrial superoxide oxidation to assess mitochondrial ROS formation, and confirmed that enhanced oxidative phosphorylation led to mitochondrial-mediated ROS production (Figure 4B).

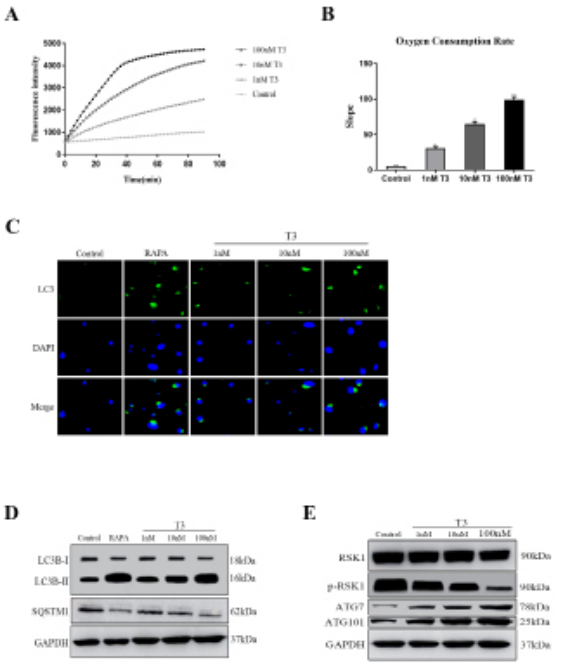


Figure 3. *Enhanced oxidative phosphorylation induces autophagy and the increased expression of ATG7 and ATG101, suppressing the activation of RSK1.*

*(A and B) Assessment of oxygen consumption rate (OCR) in T_3-treated MMQ cells at different doses for 24 hours. (C) MMQ cells were treated with different doses of T_3 for 24 hours. An Autophagy Detection Kit was used to detect autophagy in MMQ cells. Rapamycin-treated MMQ cells were used as a positive control. (D) After extraction of the proteins from MMQ cells treated with different doses of T_3 for 24 hours, Western blotting was performed using an anti-LC3B antibody and an anti-SQSTM1 antibody. Rapamycin-treated MMQ cells were used as a positive control. (E) After extraction of the proteins from MMQ cells treated with different doses of T_3 for 24 hours, Western blotting was performed using anti-RSK1, anti-phospho-RSK1, anti-ATG7, and anti-ATG101 antibodies. Bars represent the mean of the respective individual ratios ± SEM. n = 3. **- p<0.01; ***- p<0.001.*

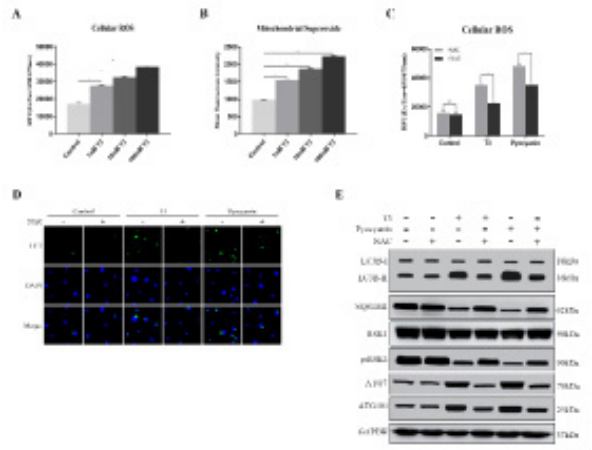


Figure 4. *Enhanced oxidative phosphorylation stimulates ROS generation, and ROS induces autophagy and the increased expression of ATG7 and ATG101, suppressing the activation of RSK1.*

*(A) Intracellular ROS generation in T_3-treated MMQ cells. (B) Mitochondrial superoxide generation in T_3-treated MMQ cells measured by MitoSOX. (C) NAC eliminated a portion of ROS in T_3 (100nM/24 h)-treated and pyocyanin-treated MMQ cells. (D) An Autophagy Detection Kit was used to detect autophagy in each group of MMQ cells. Pyocyanin-treated MMQ cells were used as a positive control. (E) After ROS were partially eliminated by NAC treatment, autophagy was decreased, the expression of ATG7 and ATG101 was decreased, and the activation of RSK1 was increased. Bars represent the mean of the respective individual ratios ± SEM. n = 3. *- p<0.05; **- p<0.01; ns - not significant.*

ROS Induce Autophagy and Increase the Expression of ATG7 and ATG101, thereby Suppressing RSK1 Activation in MMQ Cells

We next sought to verify that ROS induce autophagy and increase the expression of ATG7 and ATG101, and to suppress the activation of RSK1. We speculated that the elimination of ROS would suppress autophagy and the expression of ATG7 and ATG101, and promote RSK1 phosphorylation. The ROS scavenger NAC was used to eliminate ROS in MMQ cells, and pyocyanin, a compound known to rapidly stimulate ROS production in cells, was used as a positive control. The results in Figure 4C showed that pyocyanin stimulated MMQ cells to produce substantial amounts of ROS, and NAC treatment reduced the ROS. The results in Figure 4D showed that NAC treatment reduced LC3 fluorescence intensity in the T3- and pyocyanin-treated groups. Additionally, NAC treatment decreased LC3B-II expression and increased SQSTM1 expression in the T_3-treated and pyocyanin-treated groups (Figure 4E). In addition, NAC treatment decreased the expression of ATG7 and ATG101 and increased the expression of phospho-RSK1 in the T_3-treated and pyocyanin-treated groups (Figure 4E). Thus, NAC-mediated elimination of ROS suppressed autophagy and the expression of ATG7 and ATG101, and promoted RSK1 phosphorylation in MMQ cells. These results suggested that enhanced oxidative phosphorylation induced autophagy and increased the expression of ATG7 and ATG101, thereby suppressing the activation of RSK1 by stimulating ROS generation in MMQ cells.

The Role of Autophagy in MMQ Cells

We further investigated the role of autophagy in MMQ cells. We divided the MMQ cells into two groups: a bromocriptine-treated group and a bromocriptine-untreated group. Bromocriptine is a kind of dopamine agonist that can suppress tumor cells of prolactinoma. For each group, we chose two autophagy activators, rapamycin and LiCl, to activate autophagy in the cells, and two autophagy inhibitors, chloroquine and 3-methyladenine, to inhibit autophagy in the cells. The results of the CCK-8 assay showed that in the bromocriptine-untreated group, cell viability increased after autophagy activation; after autophagy inhibition, cell viability decreased (Figure 5A), and the results were identical in the bromocriptine-treated group (Figure 5B). The results of the BrdU assay showed that in the bromocriptine-untreated group, proliferation increased after autophagy activation; after autophagy inhibition, proliferation decreased (Figure 5C), and the results were identical in the bromocriptine-treated group (Figure 5D). We also measured prolactin production in the supernatant of MMQ cells. The results showed that in the bromocriptine-untreated group, prolactin concentration increased after autophagy activation; after autophagy inhibition, it decreased (Figure 5E), and the results were identical in the bromocriptine-treated group (Figure 5F). Based on these results, we discovered that autophagy played a protective role in MMQ cells, enhancing cell viability and proliferation and increasing prolactin secretion under both normal and pharmacological inhibition conditions.

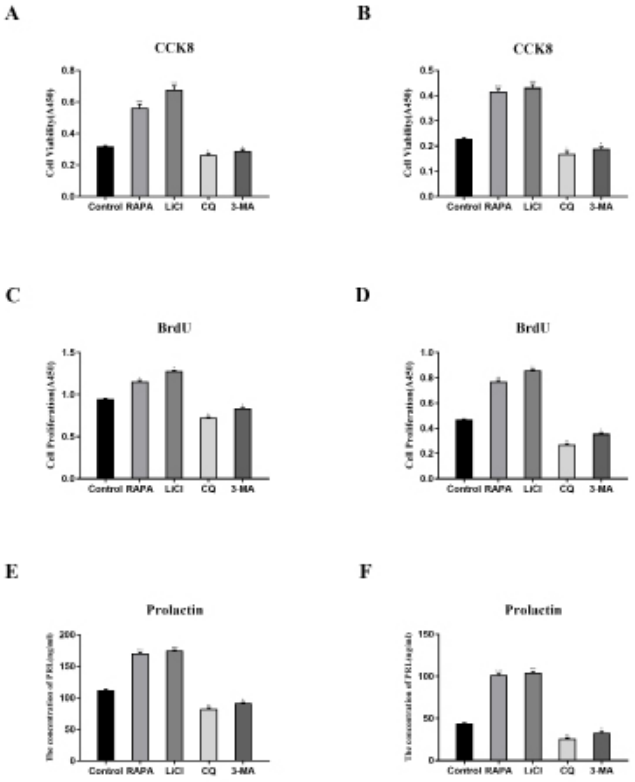


Figure 5. *The role of autophagy in MMQ cells.*

*(A) In the bromocriptine-untreated group, cell viability was enhanced after autophagy was activated by rapamycin and LiCl treatment, and the cell viability was reduced after autophagy was inhibited by chloroquine and 3-methyladenine treatment. (B) In the bromocriptine-treated group, cell viability was enhanced after autophagy was activated by rapamycin and LiCl treatment, and cell viability was reduced after autophagy was inhibited by chloroquine and 3-methyladenine treatment. (C) In the bromocriptine-untreated group, proliferation was enhanced after autophagy was activated by rapamycin and LiCl treatment, and proliferation was reduced after autophagy was inhibited by chloroquine and 3-methyladenine treatment. (D) In the bromocriptine-treated group, proliferation was enhanced after autophagy was activated by rapamycin and LiCl treatment, and proliferation was reduced after autophagy was inhibited by chloroquine and 3-methyladenine treatment. (E) In the bromocriptine-untreated group, the concentration of prolactin was increased after autophagy was activated by rapamycin and LiCl treatment, and the concentration of prolactin was decreased after autophagy was inhibited by chloroquine and 3-methyladenine treatment. (F) In the bromocriptine-treated group, the concentration of prolactin was increased after autophagy was activated by rapamycin and LiCl treatment, and the concentration of prolactin was decreased after autophagy was inhibited by chloroquine and 3-methyladenine treatment. Bars represent the mean of the respective individual ratios ± SEM. n = 3. *- p<0.05; **- p<0.01; ***- p<0.001.*

Discussion

The study of autophagy is extensive and in-depth, and a key aspect of autophagy research is the study of regulatory mechanisms.[28] Oxidative phosphorylation is a vital process in the energy production of aerobic cells, accounting for approximately 90% of adenosine triphosphate (ATP) generation during catabolism.[29] Bartolomé A et al. reported that autophagy is induced after uncoupling of oxidative phosphorylation in MEFs.[30] However, whether changes in

oxidative phosphorylation in prolactinomas induce autophagy is unclear.

In this study, we show that prolactinomas exhibit increased LC3-II expression and reduced SQSTM1 expression, indicating autophagy activation. Additionally, we show that prolactinomas have increased activity of respiratory chain complexes I, III, and IV. These results indicate that oxidative phosphorylation is enhanced in prolactinomas due to active mitochondrial function. The respiratory chain complexes I and III are the primary sources of ROS.[26] Thus, the active respiratory chain complexes I and III may cause ROS accumulation in tumor cells. Furthermore, we detected upregulation of ATG7 and ATG101 and downregulation of RSK1, according to the microarray results. The Western blot assay demonstrated that the expression of ATG7 and ATG101 was upregulated, and that the expression of RSK1 was downregulated, in prolactinomas. Next, we artificially enhanced oxidative phosphorylation in MMQ cells using T_3 and found that autophagy was activated and ROS generation increased accordingly. We also found that after oxidative phosphorylation was enhanced, the expression of ATG7 and ATG101 increased; the expression of RSK1 did not change; however, the expression of phospho-RSK1, the active form of RSK1, decreased, suggesting that RSK1 activation was suppressed. Then, we used NAC to reduce ROS levels in MMQ cells and found that, compared with the NAC-untreated group, autophagy was suppressed, and the expression of ATG7 and ATG101 was decreased in the NAC-treated group. In addition, RSK1 expression did not change significantly, whereas phospho-RSK1 expression increased, suggesting that RSK1 was activated in the NAC-treated group.

mTOR is a downstream effector molecule regulated by many signaling pathways, such as PI3K/Akt, AMPK, MAPK, and P53, and plays a significant regulatory role in tumor cells. The mTOR pathway is a common signaling pathway in autophagy, and extensive reports indicate that mTORC1, one of the mTOR complexes, is a major negative regulator of autophagy.[31-33] TSC2 is involved in the mTOR pathway and negatively regulates mTORC1,[34] and RSK1 directly phosphorylates TSC2 and potently inhibits its activity.[27] In summary, RSK1 is a negative regulator of autophagy. In prolactinomas, our results show that RSK1 and its active form, phospho-RSK1, are downregulated. In MMQ cells, although RSK1 expression is not markedly altered, its activation is suppressed.

ATG7 and ATG101 are essential molecules for autophagy; their roles in the process of autophagy have been clearly described.[7-10] Zhu J et al. reported that ATG7-mediated autophagy is a key player in regulating bladder cancer invasion,[35] and Lévy J et al. reported that the inactivation of ATG7 in intestinal epithelial cells inhibits the formation of precancerous lesions.[36] Additionally, Wei H et al. reported that knockout of FIP200, a component of the ULK1-ATG13-FIP200-ATG101 complex, significantly suppresses mammary tumorigenesis and progression in a mouse model of human breast cancer.[37] Our results show that the expression of ATG7 and ATG101 is upregulated in prolactinomas, and that their expression is increased while oxidative phosphorylation is enhanced in MMQ cells. We think that the increased expression of ATG7 and ATG101 is due to RSK1 suppression and leads to autophagy activation in prolactinomas; the underlying mechanism remains to be further explored.

ROS are a group of molecules including superoxide anions ($O_2^{\cdot-}$), hydroxyl radicals ($OH\cdot$), and hydrogen peroxide (H_2O_2). These molecules are synthesized within cells through oxygen metabolism and serve as important signaling molecules at low levels.[38] Mitochondria produce the majority of intracellular ROS through electron leakage from the electron transport chain during oxidative phosphorylation.[39,40] It is generally accepted that ROS induce autophagy.[41,42] Our findings demonstrate that ROS induce autophagy and suppress RSK1 activation in MMQ cells. However, we have not identified the relationship between ROS accumulation and RSK1 suppression in this study, and we need to conduct further research into the specific mechanism.

We further explored the role of autophagy in MMQ cells. Interestingly, we discovered that in both the bromocriptine-untreated and bromocriptine-treated groups, autophagy enhanced cell viability and proliferation and increased prolactin secretion. Recent studies have demonstrated that tumor resistance to anticancer therapies, including chemotherapy, radiation therapy, and targeted therapy, can be enhanced by upregulation of autophagy in various tumor cell lines.[43,44] Furthermore, growing evidence indicates that autophagy inhibition augments cytotoxicity when combined with several anticancer drugs in preclinical models.[45-47] Dopamine agonists have become the initial therapy for most patients with prolactinomas since they are found to be successful in reducing prolactin levels and reducing the tumor size. However, there are still some patients who do not respond to dopamine agonists satisfactorily even at considerably high doses; in other words, they display a pharmacological resistance to the function of these drugs.[48,49] Although resistant tumors appear to have fewer D_2 receptors, based on our experimental results, we speculate that the activation of autophagy in prolactinomas contributes to resistance to dopamine agonists. Furthermore, the recurrence rate of pituitary adenomas differs between subtypes, being highest in prolactinomas, with the highest incidence of recurrence occurring between 1 and 5 years after surgery.[50] We speculate that the activation of autophagy in prolactinomas is also associated with the high recurrence rate since autophagy plays a protective role in MMQ cells.

In conclusion, our findings provide a novel perspective that couples oxidative phosphorylation with autophagy, in which ROS play a pivotal role in linking these two biological functions in prolactinomas.

Acknowledgments

The author deeply and sincerely appreciates Beijing Tiantan Hospital and Tianjin First Central Hospital for providing prolactinoma and normal pituitary tissue samples.

Sources of Funding

This research received no specific grant from any funding agency in the public, commercial, or not-for-profit sectors.

Disclosure and Conflicts of Interest

The author declares no conflicts of interest.

References

1. Gillam MP, Molitch ME, Lombardi G, Colao A. Advances in the treatment of prolactinomas. Endocr Rev. 2006;27(5):485-534.
2. White E, Mehnert JM, Chan CS. Autophagy, Metabolism, and Cancer. Clin Cancer Res. 2015;21(22):5037-46.
3. Sui X, Chen R, Wang Z, Huang Z, Kong N, Zhang M, et al. Autophagy and chemotherapy resistance: a promising therapeutic target for cancer treatment. Cell Death Dis. 2013;4:e838.
4. Mowers EE, Sharifi MN, Macleod KF. Functions of autophagy in the tumor microenvironment and cancer metastasis. FEBS J. 2018;285(10):1751-66.
5. Lim KH, Staudt LM. Toll-like receptor signaling. Cold Spring Harb Perspect Biol. 2013;5(1):a011247.
6. Salminen A, Kaarniranta K, Kauppinen A. Beclin 1 interactome controls the crosstalk between apoptosis, autophagy and inflammasome activation: impact on the aging process. Ageing Res Rev. 2013;12(2):520-34.
7. Xiong J. Atg7 in development and disease: panacea or Pandora's Box? Protein Cell. 2015;6(10):722-34.
8. Noda NN, Mizushima N. Atg101: Not Just an Accessory Subunit in the Autophagy-initiation Complex. Cell Struct Funct. 2016;41(1):13-20.
9. Tanida I, Mizushima N, Kiyooka M, Ohsumi M, Ueno T, Ohsumi Y, et al. Apg7p/Cvt2p: A novel protein-activating enzyme essential for autophagy. Mol Biol Cell. 1999;10(5):1367-79.
10. Mercer CA, Kaliappan A, Dennis PB. A novel, human Atg13 binding protein, Atg101, interacts with ULK1 and is essential for macroautophagy. Autophagy. 2014;5(5):649-62.
11. Hanahan D, Weinberg RA. Hallmarks of cancer: the next generation. Cell. 2011;144(5):646-74.
12. Boroughs LK, DeBerardinis RJ. Metabolic pathways promoting cancer cell survival and growth. Nat Cell Biol. 2015;17(4):351-9.
13. Pavlova NN, Thompson CB. The Emerging Hallmarks of Cancer Metabolism. Cell Metab. 2016;23(1):27-47.
14. Hsu PP, Sabatini DM. Cancer cell metabolism: Warburg and beyond. Cell. 2008;134(5):703-7.
15. Mathupala SP, Ko YH, Pedersen PL. The pivotal roles of mitochondria in cancer: Warburg and beyond and encouraging prospects for effective therapies. Biochim Biophys Acta. 2010;1797(6-7):1225-30.
16. LeBleu VS, O'Connell JT, Gonzalez Herrera KN, Wikman H, Pantel K, Haigis MC, et al. PGC-1alpha mediates mitochondrial biogenesis and oxidative phosphorylation in cancer cells to promote metastasis. Nat Cell Biol. 2014;16(10):992-1003, 1-15.
17. Jiang L, Xiao L, Sugiura H, Huang X, Ali A, Kuro-o M, et al. Metabolic reprogramming during TGFbeta1-induced epithelial-to-mesenchymal transition. Oncogene. 2015;34(30):3908-16.
18. Viale A, Corti D, Draetta GF. Tumors and mitochondrial respiration: a neglected connection. Cancer Res. 2015;75(18):3685-6.
19. Viale A, Pettazzoni P, Lyssiotis CA, Ying H, Sanchez N, Marchesini M, et al. Oncogene ablation-resistant pancreatic cancer cells depend on mitochondrial function. Nature. 2014;514(7524):628-32.
20. Roesch A, Vultur A, Bogeski I, Wang H, Zimmermann Katharina M, Speicher D, et al. Overcoming Intrinsic Multidrug Resistance in Melanoma by Blocking the Mitochondrial Respiratory Chain of Slow-Cycling JARID1Bhigh Cells. Cancer Cell. 2013;23(6):811-25.
21. Strohecker AM, White E. Targeting mitochondrial metabolism by inhibiting autophagy in BRAF-driven cancers. Cancer Discov. 2014;4(7):766-72.
22. Lu CL, Qin L, Liu HC, Candas D, Fan M, Li JJ. Tumor cells switch to mitochondrial oxidative phosphorylation under radiation via mTOR-mediated hexokinase II inhibition--a Warburg-reversing effect. PLoS One. 2015;10(3):e0121046.
23. Maiuri MC, Kroemer G. Essential role for oxidative phosphorylation in cancer progression. Cell Metab. 2015;21(1):11-2.
24. Tan AS, Baty JW, Dong LF, Bezawork-Geleta A, Endaya B, Goodwin J, et al. Mitochondrial genome acquisition restores respiratory function and tumorigenic potential of cancer cells without mitochondrial DNA. Cell Metab. 2015;21(1):81-94.
25. Xu Q, Biener-Ramanujan E, Yang W, Ramanujan VK. Targeting metabolic plasticity in breast cancer cells via mitochondrial complex I modulation. Breast Cancer Res Treat. 2015;150(1):43-56.
26. Turrens JF. Mitochondrial formation of reactive oxygen species. J Physiol. 2003;552(Pt 2):335-44.
27. Roux PP, Ballif BA, Anjum R, Gygi SP, Blenis J. Tumor-promoting phorbol esters and activated Ras inactivate the tuberous sclerosis tumor suppressor complex via p90 ribosomal S6 kinase. Proc Natl Acad Sci U S A. 2004;101(37):13489-94.
28. Abada A, Elazar Z. Getting ready for building: signaling and autophagosome biogenesis. EMBO Rep. 2014;15(8):839-52.
29. Lehninger AL, Wadkins CL, Cooper C, Devlin TM, Gamble JL. Oxidative phosphorylation. Science. 1958;128(3322):450-6.
30. Bartolomé A, García-Aguilar A, Asahara SI, Kido Y, Guillén C, Pajvani UB, et al. MTORC1 Regulates both General Autophagy and Mitophagy Induction after Oxidative Phosphorylation Uncoupling. Molecular and cellular biology. 2017;37(23).
31. Yorimitsu T, Klionsky DJ. Autophagy: molecular machinery for self-eating. Cell Death Differ. 2005;12 Suppl 2:1542-52.
32. Rubinsztein DC, Gestwicki JE, Murphy LO, Klionsky DJ. Potential therapeutic applications of autophagy. Nat Rev Drug Discov. 2007;6(4):304-12.
33. Pattingre S, Espert L, Biard-Piechaczyk M, Codogno P. Regulation of macroautophagy by mTOR and Beclin 1 complexes. Biochimie. 2008;90(2):313-23.
34. Tee AR, Fingar DC, Manning BD, Kwiatkowski DJ, Cantley LC, Blenis J. Tuberous sclerosis complex-1 and -2 gene products function together to inhibit mammalian target of rapamycin (mTOR)-mediated downstream signaling. Proc Natl Acad Sci U S A. 2002;99(21):13571-6.
35. Zhu J, Tian Z, Li Y, Hua X, Zhang D, Li J, et al. ATG7 Promotes Bladder Cancer Invasion via Autophagy-Mediated Increased ARHGDIB mRNA Stability. Adv Sci (Weinh). 2019;6(8):1801927.

36. Levy J, Cacheux W, Bara MA, L'Hermitte A, Lepage P, Fraudeau M, et al. Intestinal inhibition of Atg7 prevents tumour initiation through a microbiome-influenced immune response and suppresses tumour growth. Nat Cell Biol. 2015;17(8):1062-73.
37. Wei H, Guan JL. Pro-tumorigenic function of autophagy in mammary oncogenesis. Autophagy. 2012;8(1):129-31.
38. Gough DR, Cotter TG. Hydrogen peroxide: a Jekyll and Hyde signalling molecule. Cell Death Dis. 2011;2:e213.
39. St-Pierre J, Buckingham JA, Roebuck SJ, Brand MD. Topology of superoxide production from different sites in the mitochondrial electron transport chain. J Biol Chem. 2002;277(47):44784-90.
40. Murphy MP. How mitochondria produce reactive oxygen species. Biochem J. 2009;417(1):1-13.
41. Azad MB, Chen Y, Gibson SB. Regulation of autophagy by reactive oxygen species (ROS): implications for cancer progression and treatment. Antioxid Redox Signal. 2009;11(4):777-90.
42. Moore MN. Autophagy as a second level protective process in conferring resistance to environmentally-induced oxidative stress. Autophagy. 2008;4(2):254-6.
43. Hu YL, Jahangiri A, Delay M, Aghi MK. Tumor cell autophagy as an adaptive response mediating resistance to treatments such as antiangiogenic therapy. Cancer Res. 2012;72(17):4294-9.
44. Zou Z, Yuan Z, Zhang Q, Long Z, Chen J, Tang Z, et al. Aurora kinase A inhibition-induced autophagy triggers drug resistance in breast cancer cells. Autophagy. 2012;8(12):1798-810.
45. Firat E, Weyerbrock A, Gaedicke S, Grosu AL, Niedermann GJPO. Chloroquine or Chloroquine-PI3K/Akt Pathway Inhibitor Combinations Strongly Promote γ-Irradiation-Induced Cell Death in Primary Stem-Like Glioma Cells. 2012;7(10):e47357.
46. Carew JS, Nawrocki ST, Kahue CN, Zhang H, Yang C, Chung L, et al. Targeting autophagy augments the anticancer activity of the histone deacetylase inhibitor SAHA to overcome Bcr-Abl-mediated drug resistance. Blood. 2007;110(1):313-22.
47. Sotelo J, Briceño E, López-González MA. Adding chloroquine to conventional treatment for glioblastoma multiforme: a randomized, double-blind, placebo-controlled trial. Annals of internal medicine. 2006;144(5):337-43.
48. Molitch ME. Dopamine resistance of prolactinomas. Pituitary. 2003;6(1):19-27.
49. Soule SG, Powell M, Jacobs HS. Prolactinomas resistant to dopamine agonists: insights into pathogenesis and therapy. Current opinion in obstetrics & gynecology. 1994;6(4):393-7.
50. Roelfsema F, Biermasz NR, Pereira AM. Clinical factors involved in the recurrence of pituitary adenomas after surgical remission: a structured review and meta-analysis. Pituitary. 2012;15(1):71-83.

***Corresponding author*: *Yutao Shen; Email: hzabcsyt@163.com; Address: No. 525, Liuhe Road, Xihu District, Hangzhou 310023, Zhejiang, China.*

Supplementary Table 1. The 2,481 genes differentially expressed between prolactinoma and normal pituitary samples.

Supplementary Table 2. The result of KEGG analysis of 2,481 differentially expressed genes.